



Development of Silymarin Entrapped Chitosan Phthalate Nanoparticles for Targeting Colon Cancer

U. Ubaidulla*, Priyanka Sinha, T. Sangavi and Grace Rathnam

Department of Pharmaceutics, Crescent School of Pharmacy, B. S. Abdur Rahman Crescent Institute of Science and Technology, Chennai - 600048, India; ubaidulla@crescent.education

Abstract

The present paper deals with the development of silymarin entrapped Chitosan Phthalate (CP) nanoparticles for targeting colon cancer. The QbD approach is applied to optimize the silymarin loaded chitosan phthalate nanoparticles. DOE was employed to evaluate the dependent variables from the responses of CP nanoparticles. The CP NPs were found to be 140% of mucoadhesivity at pH 7.4, superior to pH 1.2 (10%). The result revealed the chemical or ionic bond formation between the positively charged amino groups of chitosan phthalate and the negatively charged sialic acid residue of mucin present in the mucous membrane. *In vitro* drug release profiles were carried out under acidic and basic pH conditions. The release of encapsulated silymarin was found to be poor in acidic conditions and maximum in basic conditions. The results suggested that chitosan phthalate nanoparticles could have the potential to enhance the bioavailability of silymarin.

Keywords: Chitosan Phthalate, Colon Cancer, Design of Experiments (DOE), Nanoparticles, Quality by Design (QbD), Silymarin

1. Introduction

Colon cancer is the third most deadly cancer and causes ten percent of deaths globally each year. Approximately 80% of cancer patients utilise herbal drugs with chemotherapeutic medicines during the early stages of therapy. Furthermore, roughly 50% of cancer patients receive herbal medications. Concurrent therapy is increasingly being used to prevent side effects, increase immunity and improve overall health, but the possible impacts of using many medicines at the same time might be beneficial or injurious.

Active therapeutic components of the herb have influenced the public in the last 2 decades. An ancient drug *Silybum marianum* contains many flavonolignans and a group of undefined polyphenolic compounds¹. The therapeutic activity of silymarin is the synergistic action of its constituents. Silymarin has anti-angiogenic,

anti-cancer, anti-viral, and antifibrotic properties, according to research².

Although silymarin has been demonstrated to possess various pharmacological properties and is used clinically for treating liver diseases³, its poor aqueous solubility has limited its clinical applications. For enhancing bioabsorption and bioavailability of the natural drug, several strategies like solid dispersion, liposome, self-microemulsifying drug delivery systems, and mechanical activation with hydrophilic polymers have been investigated to modify the physicochemical nature of silymarin⁴. However, the therapeutic activity and drug release of the herbal drug silymarin can be improved by nanoparticles⁵. Because the system in nanoparticles can give an increase in surface area and dissolution rate, it is particularly advantageous for poorly soluble compounds. To achieve targeted drug

*Author for correspondence

release and to prevent physiological barriers, polymeric nanoparticles are widely used⁶. In the present study, chitosan phthalate polymer was synthesized using chitosan by the substituent's method for shifting the solubility of chitosan from acidic pH to basic pH. Additional advantages of chitosan are that it protects the drug from acidic environmental degradation and enhances the anti - cancer activity of silymarin.

The present investigation was designed by design software to formulate silymarin-loaded chitosan phthalate nanoparticles for targeting colon cancer. No evidence reports were available on chitosan phthalate nanoparticles containing silymarin for colon specific delivery. This has prompted us to make an attempt to develop chitosan phthalate nanoparticles as a carrier for delivering the drug at the target site.

2. Methods

2.1 FT-IR Analysis

The drug and the excipients chosen for the formulations were screened for compatibility by physical methods. The physical mixture of silymarin and excipients was analysed using FTIR spectroscopy.

2.2 Design of Experiment (DOE)

The response surface methodology was implemented as the design of the experiment and the independent variables were studied with varying concentrations of

chitosan phthalate, tripolyphosphate and stirring speed with different RPM. Particle size, entrapment efficiency and drug release were considered as dependent variables (Table 1).

The three-factor, three-level statistical screening method used to optimise the nanoparticles is called Box-Behnken Design (BBD).

2.3 Preparation of Silymarin Loaded CP Nanoparticles

Based on our previous work, Chitosan phthalate was prepared⁷. Chitosan was dissolved in an acidic solution and phthalic anhydride was added to the pyridine solution and mixed thoroughly. By the addition of NaOH, the pH was maintained at 7.0. After 1 hr, 200ml of 20% aqueous NaCl solution was added to stop the reaction. The resultant product was filtered and washed with organic solvent to remove the unreacted reactants. The silymarin loaded CP nanoparticles were formulated by the ionotropic crosslinking method. Silymarin was added to the CP solution, and the mixture was stirred for 1 hour at 1500 rpm. The chitosan phthalate/silymarin solution was added to tripolyphosphate (TPP) (10% w/v) continuously. The silymarin loaded chitosan phthalate nanoparticles were kept in the dessicator until further use (Table 2).

Response surface modelling and the ability to fit the model were evaluated with Design-Expert® software (Version 12).

Table 1. Box-Behnken experimental design

Independent factors	Unit	Levels		
		Low	Medium	High
X ₁ = Amount of chitosan phthalate	%	2	6	10
X ₂ = Amount of tripolyphosphate	%	5	10	15
X ₃ = Stirring speed	Rpm	500	1000	1500
Responses (dependent factors)				
Y1 = Size	Nanometre			
Y2 = EE of nanoparticles	%			
Y3 = Percentage of silymarin release	%			

Table 2. Formula of silymarin loaded chitosan phthalate nanoparticles

Formulation Code	Silymarin (mg)	Chitosan Phthalate (%)	Tripolyphosphate (TPP) (% w/v)	Stirring Speed (rpm)
1	10	2	5	500
2	10	2	5	1000
3	10	2	10	500
4	10	2	10	1500
5	10	2	15	100
6	10	6	5	500
7	10	6	5	1000
8	10	6	5	1500
9	10	6	10	1000
10	10	6	15	500
11	10	6	15	1000
12	10	6	15	1500
13	10	10	5	500
14	10	10	5	1000
15	10	10	5	1500
16	10	10	10	1500
17	10	10	15	1000

2.4 Characterization of Silymarin Loaded Chitosan Phthalate Nanoparticles

2.4.1 Scanning Electron Microscopy (SEM)

Scanning electron microscopy was used to investigate the structure and surface properties of silymarin nanoparticles using the gold sputtering technique (TESCAN VEGA-3, Czech Republic). CP nanoparticles were scattered with the double tape on an aluminium stub, and the stubs containing the sample were then coated with gold to a thickness of 400 Å using a cool sputter coater. Images were captured at a 20 kV accelerated voltage and a chamber pressure of 0.6 mmHg.

2.4.2 X-ray Diffraction Study

X-ray diffractometry was used to investigate the crystalline behaviour of CP nanoparticles. Diffraction patterns were acquired using the Rigaku Mini Flex II-Japan X-ray generator at 40 kV tube voltages and 35mA tube current.

2.4.3 Swelling Index

At room temperature, CP nanoparticles were submerged in pH 1.2 and pH 7.4 for 8 hours until swollen equilibrium was reached. The nanoparticles were then wiped using filter paper to remove any surface absorbed liquid before being weighed instantly. The swelling percentage was calculated as follows:
Swelling index (%) = $\frac{\text{Final weight (W}_2\text{)} - \text{Initial weight (W}_1\text{)}}{\text{Final weight (W}_2\text{)}} \times 100$

2.4.4 Mucoadhesive Study

An *in vitro* wash-off test was used to determine the mucoadhesive characteristics. The rat specimen was threaded onto a glass slide. The nanoparticles were then applied to the wet, cleaned specimen and allowed to hydrate for 30 s. The prepared slide was hung onto one of the grooves of a USP 24 tablet disintegrating test apparatus. The disintegration test apparatus was set up such that the specimen was moved up and down in a jar holding one litre of pH 7.4 at 37°C on a regular

basis. The machine was stopped and assessed after 1 h at hourly intervals up to 8 h.

$$\% \text{ Mucoadhesive strength} = P1/P2 * 100$$

Where,

P1: Amount of drug adhered

P2: Amount of drug added

2.4.5 In vitro Release Study

Using USP dissolving apparatus I, an *in vitro* drug dissolution investigation of silymarin loaded chitosan phthalate nanoparticles was performed. The dissolution test was performed using 900 ml of dissolving liquid,

pH 1.2 (0.1 N HCL) for two hours, followed by pH 7.4 (phosphate buffer) for 6 h. Throughout the experiment, the rotational speed was kept at 50 rpm and the temperature was kept at 37 ± 0.5 °C. During the investigation, 5ml of the aliquots were taken from the dissolving medium at predefined time intervals (0, 1, 2, 4, 6 and 8 hours) and replaced with fresh medium. A UV-Visible spectrophotometer was used to measure the amount of drug released at 286 nm. To explore the release mechanism, drug release data was integrated into kinetic equations (zero-order, first-order Higuchi, Hixson-Crowel, and Korsmeyer-Peppas).

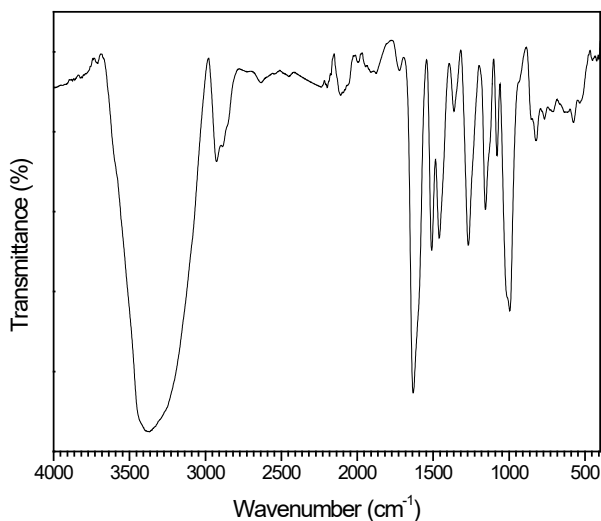


Figure 1. FTIR spectrum of silymarin.

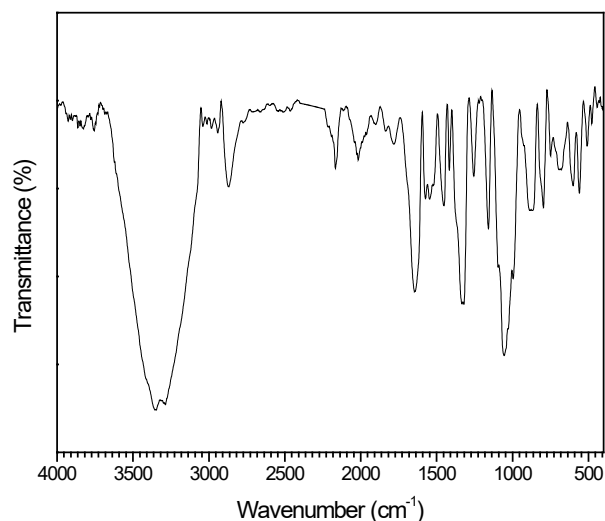


Figure 2. FTIR spectrum of chitosan.

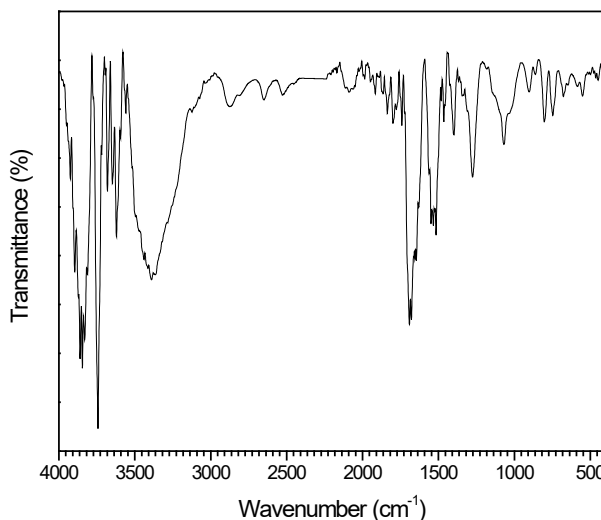


Figure 3. FTIR Spectrum of chitosan phthalate.

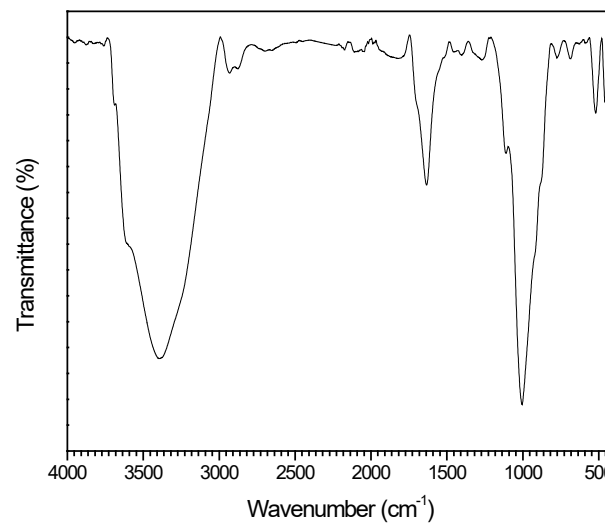


Figure 4. FTIR spectrum of silymarin loaded chitosan phthalate nanoparticles.

3. Results

3.1 FTIR Analysis

3.2 Design of Experiment (DOE)

3.2.1 Response Surface Methodology and ANOVA

Figure 5 (a), (b) and (c) depict the three-dimensional (3D) response plots showing the impact of three

variables on the response – particle size.

Figure 6 (a), (b) and (c) depict the three-dimensional 3D response plots showing the impacts of three variables on response-entrapment efficiency.

Figure 7 (a), (b) and (c) depict the three-dimensional (3D) response plots showing the impact of three variables on the response-drug release.

Design-Expert® Software
Factor Coding: Actual

Size (nm)

- Design points above predicted value
- Design points below predicted value

85 450

X1 = A: Chitosan
X2 = B: TPP

Actual Factor
C: Stirring speed = 1000

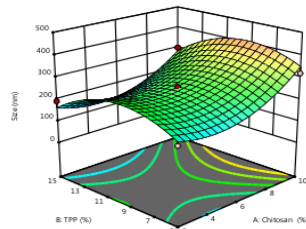


Figure 5(a). Impact of polymer and cross-linker on size of nanoparticles (nm).

Design-Expert® Software
Factor Coding: Actual

Size (nm)

- Design points above predicted value
- Design points below predicted value

85 450

X1 = A: Chitosan
X2 = C: Stirring speed

Actual Factor
B: TPP = 10

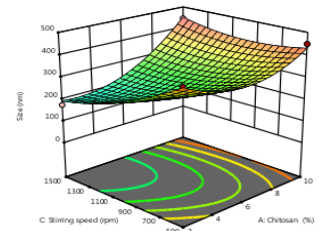


Figure 5(b). Impact of polymer and stirring speed on size of nanoparticles (nm).

Design-Expert® Software
Factor Coding: Actual

Size (nm)

- Design points above predicted value
- Design points below predicted value

85 450

X1 = B: TPP
X2 = C: Stirring speed

Actual Factor
A: Chitosan = 6

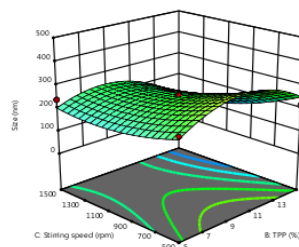


Figure 5(c). Effect of TPP concentration and stirring speed (rpm) on size of nanoparticles (nm).

Entrapment Efficiency (%)
 ● Design points above predicted value
 ○ Design points below predicted value
 30 79

X1 = A: Chitosan
 X2 = B: TPP
Actual Factor
 C: Stirring speed = 1000

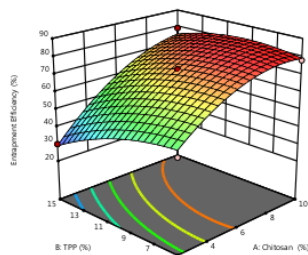


Figure 6(a). Impact of polymer and cross-linker on entrapment efficiency (%) of nanoparticles.

Design-Expert® Software
 Factor Coding: Actual
Entrapment Efficiency (%)
 ● Design points above predicted value
 ○ Design points below predicted value
 30 79

X1 = A: Chitosan
 X2 = C: Stirring speed
Actual Factor
 B: TPP = 10

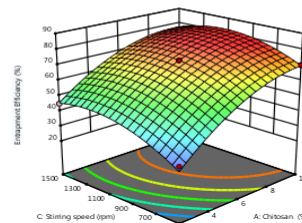


Figure 6(b). Impact of concentration of polymer and stirring speed (rpm) on entrapment efficiency (%) of the formulation.

Design-Expert® Software
 Factor Coding: Actual
Entrapment Efficiency (%)
 ● Design points above predicted value
 ○ Design points below predicted value
 30 79

X1 = B: TPP
 X2 = C: Stirring speed
Actual Factor
 A: Chitosan = 6

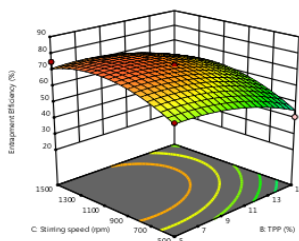


Figure 6(c). Impact of TPP and stirring speed (rpm) on entrapment efficiency (%).

Design-Expert® Software
 Factor Coding: Actual
Drug release (%)
 ● Design points above predicted value
 ○ Design points below predicted value
 50 90

X1 = A: Chitosan
 X2 = B: TPP
Actual Factor
 C: Stirring speed = 1000

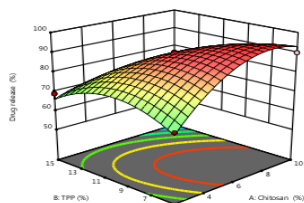


Figure 7(a). Impact of polymer and cross-linker on silymarin release.

Design-Expert® Software
 Factor Coding: Actual
Drug release (%)
 ● Design points above predicted value
 ○ Design points below predicted value
 50 90

X1 = A: Chitosan
 X2 = C: Stirring speed
Actual Factor
 B: TPP = 10

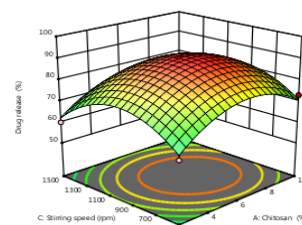


Figure 7(b). Impact of polymer concentrations and stirring speed (rpm) on silymarin releases.

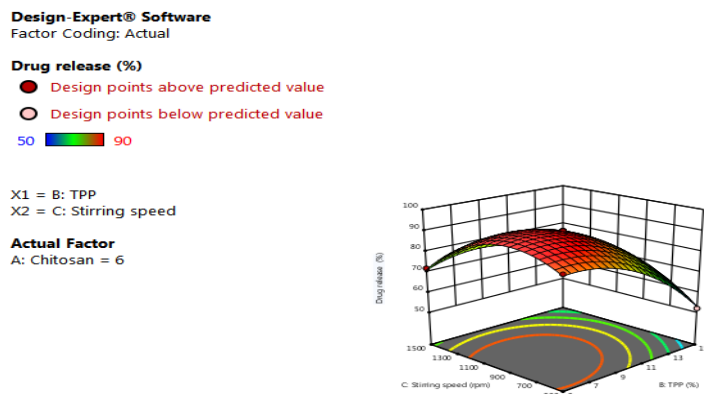


Figure 7(c). Impact of cross-linking agent and stirring speed (rpm) on silymarin release.

Table 3. Response model and statistical parameters obtained from ANOVA for BBD

Responses	Adjusted R ²	Predicted R ²	Model P value	Adequate precision	%CV
Particle size	0.9070	0.9488	<0.0004	15.57	11.03
Entrapment efficiency	0.9555	0.9345	<0.0005	18.78	5.59
Drug release	0.9713	0.7992.	<0.0001	22.15	3.31

3.2.2 Point Prediction

Table 4. Optimum formulation derived by BBD

Factor	Chitosan Phthalate (%)	TPP (%)	Stirring Speed (rpm)	Desirability
Optimum formulation	6.672	5.000	1136.38	0.952

3.2.3 Predicted and Observed Values

The experimental and predicted values along with percentage error were obtained and were tabulated in Table 5.

Table 5. Value of responses under optimal assay conditions for nanoparticles

Point Prediction	Particle size (nm)	Entrapment efficiency (%)	Drug release (%)
Predicted	204.04±1.32	76.86±0.56	86.68±0.44
Observed	217.68±0.96	81.72±0.38	95.2±1.41
% error	6.22	6.23	9.82

% error = (observed value-predicted value)/predicted value x 100

3.3 Characterization of Optimized Nanoparticles

3.3.1 Scanning Electron Microscope (SEM)

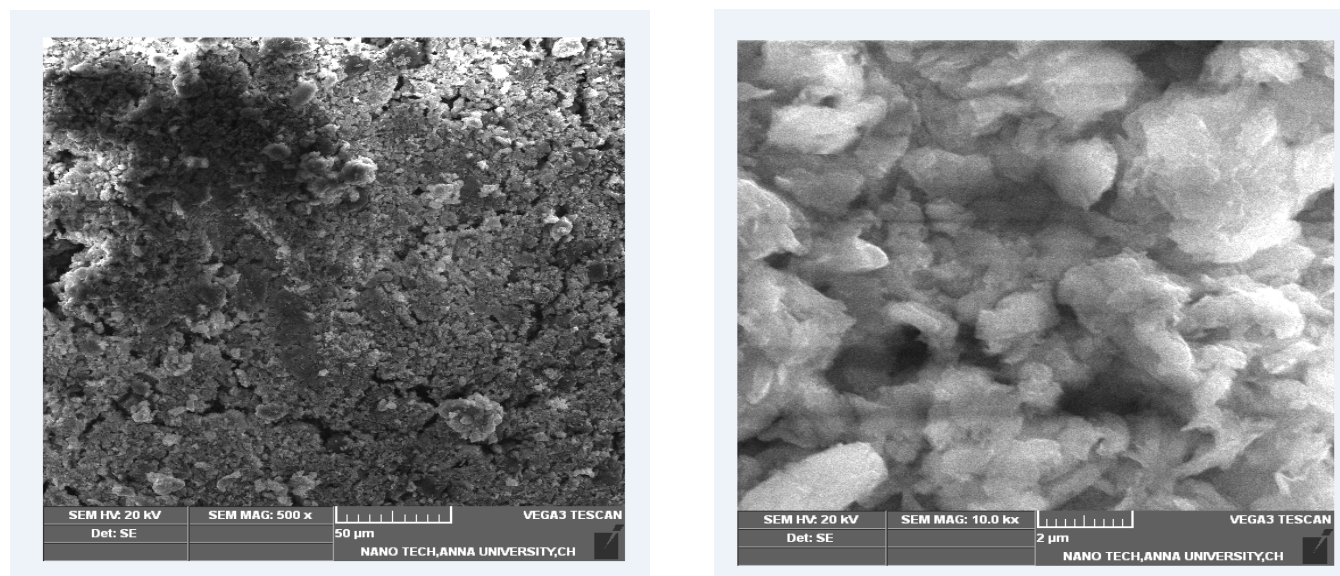


Figure 8. SEM image of silymarin loaded chitosan phthalate nanoparticles f (x10).

3.3.2 X-ray Diffraction Study

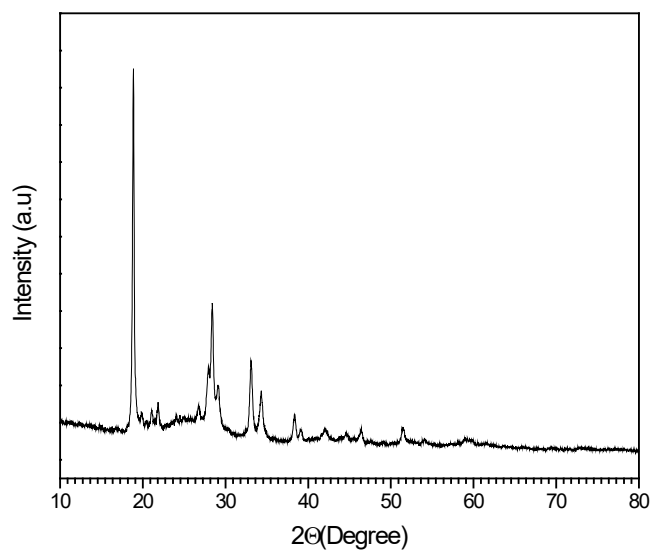


Figure 9. XRD pattern of silymarin loaded chitosan phthalate nanoparticles.

3.3.3 Swelling Index (%) of Optimized Formulation

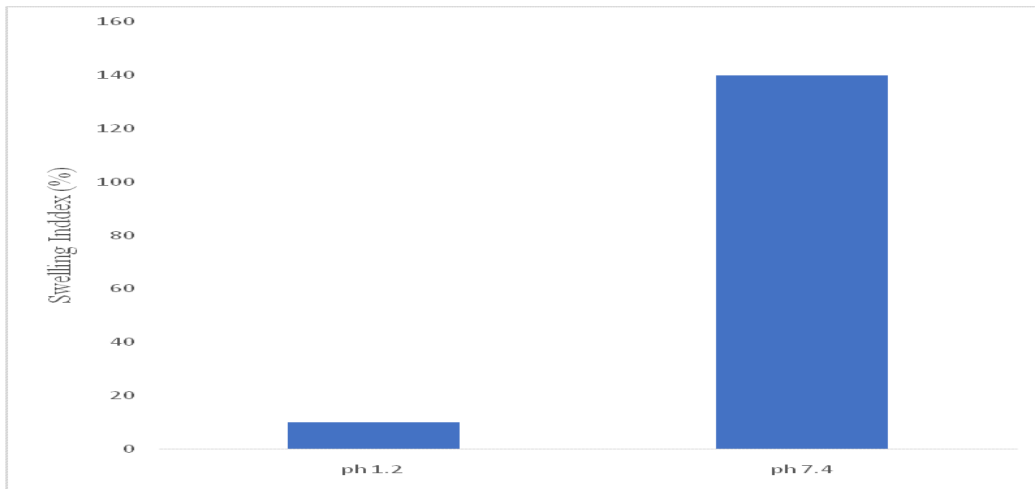


Figure 10. Swelling index (%) of optimized formulation.

3.3.4 In vitro Release of Optimized Formulation

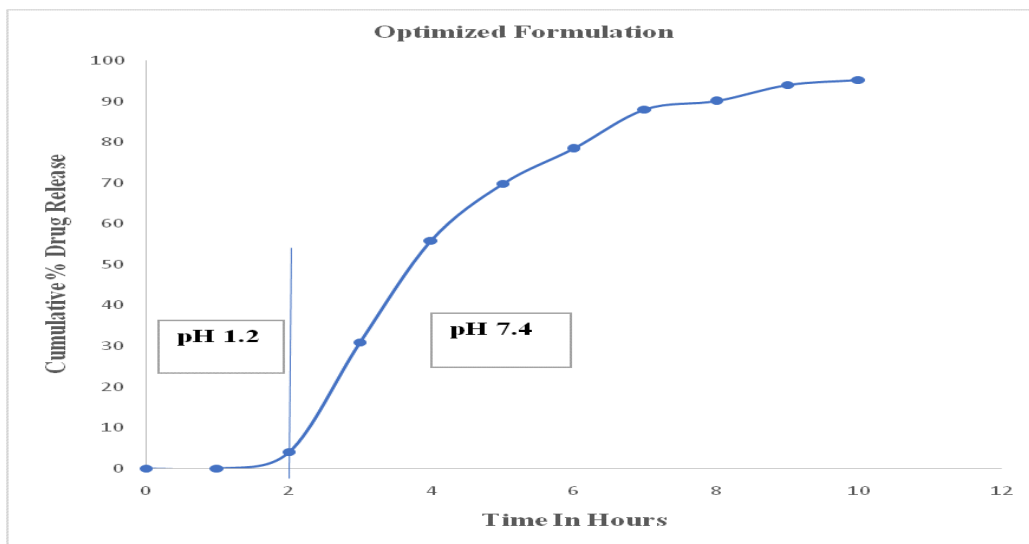


Figure 11. Silymarin release from CP nanoparticles.

3.3.5 In vitro Kinetic Analysis

Table 6. <i>In vitro</i> kinetics of optimized silymarin loaded CP nanoparticles Silymarin NPs	0 order		1st order		Higuchi kinetics		K-Peppas	
	K	r²	K	r²	K	r²	r²	n
	11.29	0.9129	-0.139	0.9722	51.72	0.9178	0.98	0.681

4. Discussion

The interaction of the drug and the excipients was studied, and the spectra of silymarin, chitosan and Chitosan Phthalate (CP) are depicted in Figures 1-4. There is no significant difference in the FTIR spectra of drugs and excipients. The FT-IR spectrum of pure silymarin exhibited a characteristic peak at 3433.4 cm^{-1} (O-H stretching vibration); 1733.6 cm^{-1} (C=O stretching vibration); and 1205.4 cm^{-1} (C-O stretching vibration); and 854.5 cm^{-1} (C-H stretching vibration) respectively. The chitosan showed the IR spectra of peaks at 3465.5 cm^{-1} (O-H stretching vibration); 2919.2 cm^{-1} (C-H stretching vibration); 1793.5 cm^{-1} (C=O stretching vibration); 1415.2 cm^{-1} , 1135.3 cm^{-1} (S=O stretching vibration); and 785.2 cm^{-1} (C-H bending vibration). The chitosan phthalate showed the IR spectra of peak at 3685.2 cm^{-1} (O-H stretching vibration); 3353.6 cm^{-1} (C-H stretching vibration); 1745.2 cm^{-1} , 1125.2 cm^{-1} (C=O stretching vibration); 745.1 cm^{-1} , (C=C bending vibration) which clearly indicate that no interaction exists between pure silymarin and excipients, it was observed that there were no change or shift in the main peaks in IR spectra of mixture of drug and excipient's. IR studies indicated no interaction between drug and excipients.

4.1 Optimization Study

Concentration of chitosan phthalate, TPP and stirring speed influenced the particle size (nm), EE (%) and release (%) of the prepared silymarin entrapped chitosan phthalate nanoparticles under optimal assay conditions. The following polynomial equation was used to optimize the parameters.

$$Y = \alpha_0 + \alpha_1 X_1 + \alpha_2 X_2 + \alpha_3 X_3 + \alpha_4 X_1 X_2 + \alpha_5 X_2 X_3 + \alpha_6 X_1 X_3 + \alpha_7 X_1^2 + \alpha_8 X_2^2 + \alpha_9 X_3^2$$

4.2 Response Surface Methodology

Figure 5(a) shows the term AB, where A is chitosan phthalate and B is TPP. As the concentration of chitosan phthalate increases, the size of the particle increases, whereas when the chitosan conc. decreases, the size of the particles decreases. On the other hand, the addition of a lower amount of TPP increases the size of particles, and when the concentration of TPP is medium, the size of the particles increases.

Figure 5(b) shows the term AC, where A is chitosan phthalate and C is the stirring speed. It is indicated that an increase in chitosan phthalate quantity leads to an increase in particle size. The size of the nanoparticles was decreased while increasing the stirring speed.

Figure 5(c) shows the term BC, where B is the concentration of TPP and C is the stirring speed. The decrease in the conc. of TPP affects the size of particles, whereas when the concentration of TPP is medium, the size increases. When the stirring speed increases, the size decreases, and on decreasing the stirring speed, the size increases.

Figure 6(a) illustrates the term AB, where A is the concentration of chitosan phthalate and B is the concentration of TPP. On decreasing the concentration of chitosan phthalate, results that entrapment efficiency was decreased. When the concentration of TPP increased, the entrapment efficiency of nanoparticles decreased. While decreasing the concentration of TPP, the entrapment efficiency increased gradually.

Figure 6(b) illustrates the term AC, where A is the concentration of chitosan phthalate and C is the stirring speed. The increase in the concentration of chitosan phthalate increases the entrapment efficiency, and the decrease in concentration of chitosan phthalate decreases the entrapment efficiency. As the rate of stirring speed increases, the entrapment efficiency also increases, and on decreasing the stirring speed, the entrapment efficiency decreases.

Figure 6(c) illustrates the term BC where B is the concentration of TPP and C is the stirring speed. As the concentration of TPP increases, the entrapment efficiency decreases, and on decreasing the concentration of TPP, the entrapment efficiency increases. Increased stirring speed, on the other hand, resulted in an increase in entrapment efficiency. When the speed decreases, the entrapment efficiency of the formulation also decreases.

Figure 7(a) shows the term AB where A is the concentration of chitosan phthalate and B is the concentration of TPP. The increase in the concentration of chitosan phthalate increases the drug release, and on decreasing the concentration of chitosan phthalate, the release decreases. On the other hand, an increase in the TPP conc. decreases the drug release and on decreasing the conc. of TPP, the drug release increases.

Figure 7(b) shows the term AC where A is the concentration of chitosan phthalate and C is the stirring speed. When the conc. of chitosan phthalate increases, drug release also increases, and on decreasing the conc. of chitosan phthalate, drug release also decreases. When the stirring speed increases, drug release also increases.

Figure 7(c) shows the term BC where B is the TPP and C is the stirring speed. When the conc. of TPP increases, drug release decreases. By the way, when the concentration of TPP decreases, drug release decreases.

4.3 ANOVA

Table 3 represents the statistical parameters such as adjusted R^2 , predicted R^2 , model P values, adequate precision, and %CV. It also shows that the adjusted R^2 for Y_1 , Y_2 and Y_3 is in good agreement with the predicted R^2 .

4.3.1 Polynomial Model Equations

The responses of Y_1 , Y_2 and Y_3 are equated and shown in Table 7.

4.3.2 Point Prediction

The silymarin-loaded chitosan phthalate nanoparticles were formulated and responses were measured. The observed values of the responses to the design were compared to the predicted values. A percentage of error was calculated to validate the method (Tables 4 and 5). The observed values of Y_1 , Y_2 and Y_3 were corroborated with predicted values. By this, the validity of the optimization procedure was proven.

An optimum CP nanoparticle may have the smallest particle size, an EE of >80%, and drug release

of >50%. Using this approach, a set of components was found. A composition of 6.672% chitosan, 5% of TPP, and 1136.88 rpm of stirring speed was predicted to have silymarin loaded chitosan phthalate nanoparticles with a particle size, EE and drug release of 205.79 nm, 82.18% and 90.00%, respectively.

Table 4 represents the desirability of CP NPs was found to be 0.952. The value falls between 0.8 and 1, which indicates the formulation quality was acceptable and excellent. If the value was <0.63, the formulation quality was considered poor^{8,9}.

4.4 Characterization of Optimized Nanoparticles

4.4.1 Scanning Electron Microscope (SEM)

A SEM image of silymarin loaded chitosan phthalate nanoparticles of different magnifications was depicted in Figure 8. SEM images were analysed at different magnifications. The spherical structure of nanoparticles was observed, which indicates good crosslinking of chitosan phthalate with TPP.

4.4.2 X-ray Diffraction Study

Pure drugs exhibited many intense and sharp diffraction angles of 20.1°, 25.3°, 29.4°, 35.9°, 40.9° and 45.7°. The chitosan when subjected to XRD showed sharp, intense peaks at 2θ value of 20.5° and chitosan phthalate showed 21.9° and 43.5°. While silymarin loaded chitosan phthalate nanoparticles depicted peaks at 19.9°, 27.4°, 33.9°, 39.4° and 46.5° which were shown in Figure 9.

Table 7. Polynomial model equations

Polynomial model	
Particle size (Y_1)	+258+70.36*A-25.75*B-50.00*C-7.75*AB+59.75*AC-26.75*BC+81.63*A ² -91.88*B ² +33.12*C ²
Entrapment efficiency (Y_2)	+81.12+18.12*A-6.88*B+6.00*C+4.32*AB-1.98*AC+2.02*BC-7.88*A ² -6.07*B ²
Drug release (Y_3)	+95.2+2.88*A-10.63*B-2.31*C-10.25*AB-0.500*AC+5.50*BC-11.13*A ² -9.63*B ²

4.4.3 Mucoadhesive Study (%)

The mucoadhesion test for optimized silymarin loaded chitosan phthalate nanoparticles was performed at pH 7.4 and was found to have 45% of nanoparticles adhered to the surface of the membrane at the end of the test. The result revealed that the interaction of amino groups of chitosan phthalate (+ charge) and sialic acid residue of mucin (- charge) resulted in the formation of bonds which could provide strong mucoadhesive behaviour.

4.4.4 Swelling Index (%) of Optimized Formulation

The effect of pH on the swelling of silymarin entrapped CP NPs is represented in Figure 10. The swelling index of nanoparticles at pH 1.2 is 10% and at pH 7.4 the swelling index is 140%. The results revealed that the swelling capacity of nanoparticles may be poor in acidic media. The result revealed that the polymer has carboxylic groups in nonionised under acidic resulting in a poorly hydrophilic result whereas carboxylic groups exist in ionized form and are considerably hydrophilic at alkaline pH. The CP NPs may not release the silymarin in the acidic pH condition of the stomach.

4.4.5 In vitro Release of Optimized Formulation

The *in vitro* release of the optimized formulation was depicted in Figure 11. The maximum release of silymarin from the CP NPs at pH 7.4 portrayed the *in vitro* drug release of silymarin loaded chitosan phthalate nanoparticles. The results revealed that the hydrophilic characteristics of the polymer predominated due to the formation of carboxylate anions. The *in vitro* release profile of silymarin obviously indicated that the drug release rates were inversely proportional to the amount of polymer in nanoparticles. Various ratios of CP and TPP were applied to achieve the release rate. Polymer and cross-linker concentration play a role in controlling the drug release from the nanoparticles by altering the diffusion path length for the drug.

4.4.6 In vitro Kinetic Analysis

The release profile of CP NPs was fitted to various models (0 orders, 1st order, Higuchi and KP) in order to study the release kinetics mechanism. Accordingly,

the optimized formulation fitted with all dissolution models and the values were shown in Table 6. A good correlation co-efficient ($r^2 < 0.9178$) was found in Higuchi kinetics, which indicates optimum dominated mechanism¹⁰. The release exponent of the Peppas model ($n < 0.7$) indicates anomalous (non-fickian) transport and rates as a function of time follow zero-order release.

5. Conclusion

Silymarin loaded chitosan phthalate nanoparticles were prepared and optimized using the Box-Behnken Design model. From the desirability function, the amount of chitosan phthalate, TPP and stirring speed were optimized with values of 6.672%, 5.0% and 1136.38 rpm with a desirability of 0.952 respectively. The swellability of nanoparticles was found to be high at pH 7.4, whereas at pH 1.2 the swelling index was found to be low. The mucoadhesivity of silymarin loaded chitosan phthalate nanoparticles was found to be good on rat tissue membrane. The *in vitro* release of CP NPs showed a controlled manner. From the above results, it can be concluded that the silymarin loaded chitosan phthalate nanoparticles have promising drug delivery for targeting colon cancer.

6. References

1. Dixit N, Baboota S, Kohli K, Ahmad S, Ali J. Silymarin: A review of pharmacological aspects and bioavailability enhancement approaches. *Indian J Pharmacol.* 2007; 39(4):172-179. <https://doi.org/10.4103/0253-7613.36534>
2. Karimi G, Vahabzadeh M, Lari P, Rashedinia M, Moshiri M. "Silymarin", a Promising Pharmacological Agent for Treatment of Diseases. *Iran J Basic Med Sci.* 2011; 14(4):308-317.
3. Abdullah AS, Ibrahim El Tantawy El Sayed, Moneim AA, El-Torgoman, Alghamdi NA, Ullah S, Wageh S. Preparation and Characterization of Silymarin-Conjugated Gold Nanoparticles with Enhanced Anti-Fibrotic Therapeutic Effects against Hepatic Fibrosis in Rats: Role of MicroRNAs as Molecular Targets. *Biomedicines.* 2021; 9:1767. <https://doi.org/10.3390/biomedicines9121767>
4. Costanzo AD, Angelico R. Formulation Strategies for Enhancing the Bioavailability of Silymarin: The State of the

- Art. Molecules. 2019; 24:2155. <https://doi.org/10.3390/molecules24112155>
5. Yang G. Improved dissolution and bioavailability of silymarin delivered by a solid dispersion prepared using supercritical fluids. *Asian J. Pharma. Sci.* 2015; 10(3):194-202. <https://doi.org/10.1016/j.ajps.2014.12.001>
 6. El-Nahas AE, Allam AN, Abdelmonsif DA, El-Kamel AH. Silymarin-Loaded Eudragit Nanoparticles: Formulation, Characterization, and Hepatoprotective and Toxicity Evaluation. *AAPS PharmSciTech.* 2017; 18(8):3076-3086. <https://doi.org/10.1208/s12249-017-0799-9>
 7. Dasari SK, Rathnam G, Ubaidulla U, Ganesh M, Jang HT. Chitosan phthalate: A novel polymer for the multiparticulate drug delivery system for diclofenac sodium. *Adv. Polym. Technol.* 2018; 37:2013-2020. <https://doi.org/10.1002/adv.21859>
 8. U. Ubaidulla, F. J. Ahmad, R. K. Khar, P Tripathi. Optimization of chitosan succinate and chitosan phthalate microspheres for oral delivery of insulin using response surface methodology. *Pharm Dev Technol.* 2008; 14(1):99-108. <https://doi.org/10.1080/10837450802409461>
 9. Sinha P, Udhumansha U, Rathnam G, Ganesh M, Jang HT. Capecitabine Encapsulated Chitosan Succinate-Sodium Alginate Macromolecular Complex Beads For Colon Cancer Targeted Delivery: In Vitro Evaluation. *Int. J. Biol. Macromol.* 2018; 117:840-850. <https://doi.org/10.1016/j.ijbiomac.2018.05.181>
 10. Ganesh M, Ubaidulla U, Rathnam G, Jang HT. Chitosan-Telmisartan polymeric cocrystals for improving oral absorption: In vitro and in vivo evaluation. *Int. J. Biol. Macromol.* 2019; 131:879-885. <https://doi.org/10.1016/j.ijbiomac.2019.03.141>